Crystal Structure of the Mutant Yeast Triosephosphate Isomerase in Which the Catalytic Base Glutamic Acid 165 Is Changed to Aspartic Acid†

Diane Joseph-McCarthy,‡,§ Linda E. Rost,‖ Elizabeth A. Komives,⊥,# and Gregory A. Petsko*,△

Departments of Biology, Biochemistry, and Chemistry, Rosenstiel Basic Medical Sciences Research Center, Brandeis University, Waltham, Massachusetts 02254-9110, Departments of Chemistry and Biochemistry, Harvard University, Cambridge, Massachusetts 02138, and Department of Chemistry, Massachusetts Institute of Technology, Cambridge, Massachusetts 02139

Received August 5, 1993; Revised Manuscript Received October 28, 1993•

ABSTRACT: The three-dimensional structure of the E165D mutant of the glycolytic enzyme yeast triosephosphate isomerase has been determined by X-ray diffraction at a nominal resolution of 2 Å. For crystallization, the mutant enzyme was complexed with the tight-binding intermediate analog, phosphoglycolohydroxamate. Comparison with the structure of the wild-type enzyme reveals that, as originally intended, replacement of the catalytic base Glu-165 with the shorter side chain of aspartic acid has increased the distance between the base and the intermediate analog by 1 Å. In addition, the catalytic base is oriented in the E165D structure so as to use the *anti* orbital of the carboxylate for proton abstraction; in the structure of the wild-type enzyme, the *syn* orbital is oriented for this purpose. It has been hypothesized that the 1000-fold loss in catalytic activity for this mutant triosephosphate isomerase is due either to the use of the less basic *anti* orbital for proton transfer or to the greater distance between the base and the substrate. The structure of yeast E165D triosephosphate isomerase suggests that both distance and orientation factors contribute to the loss of activity in the mutant enzyme and, therefore, that both factors contribute to the catalytic efficiency of the wild-type enzyme.

Triosephosphate isomerase (TIM, EC 5.3.1.1) is a dimeric glycolytic enzyme that catalyzes the interconversion of the two products of the aldolase reaction, dihydroxyacetone phosphate (DHAP) and D-glyceraldehyde 3-phosphate (GAP). The kinetics of catalysis was analyzed by Albery, Knowles, and co-workers, from which the free energy profile of the enzymatic reaction could be derived (Albery & Knowles, 1976a,b). The results from these studies suggest that TIM has reached evolutionary perfection as a catalyst (Knowles & Albery, 1977), i.e., there is no selective pressure for further improvement in the catalytic rate, which is limited solely by the diffusion of substrate to the active site (Blacklow et al., 1988).

A variety of techniques has been used to probe the structural basis for the catalytic efficiency of TIM. Active-site-directed electrophilic reagents specifically labeled the carboxylate of Glu-165 (Hartman, 1968), identifying this as a catalytic base. Additional studies (Webb & Knowles, 1974; Belasco & Knowles, 1980) have suggested the presence of an electrophilic catalyst in the active site. These studies were confirmed by the X-ray structures of native chicken TIM (Phillips et al., 1977) and native yeast TIM (Alber et al., 1981). Crystallographic studies also revealed a large conformational change in a surface loop near the active site when substrate and competitive inhibitors were diffused into the native crystal forms.

From these studies, a detailed mechanism (Knowles, 1991) has been proposed for the TIM-catalyzed isomerization (Figure 1), involving the basic carboxylate of Glu-165 (Hermes et al., 1987; Alber et al., 1987), the electrophilic participation of His-95 (Komives et al., 1991), and possibly electrostatic substrate polarization by Lys-12 [Joseph-McCarthy et al. (1994) preceding article in this issue] and two α-helix dipoles (Lodi & Knowles, 1993). As a first test of this mechanism, Knowles and co-workers used site-directed mutagenesis to change Glu-165 to aspartic acid (Straus et al., 1985). This mutation was designed to separate the catalytic base from the substrate by about 1 Å. Substitution of Asp for Glu in chicken TIM reduced the catalytic activity of wild-type enzyme by more than 2-fold, the predominant effect being the destabilization of the transition states for proton abstraction (Raines et al., 1986). This mutant was later used as the starting point for studies designed to probe the possible degeneracy of active-site design, and a number of pseudorevertants were found that increased k_{cat} for the E165D enzyme back toward wild-type levels (Blacklow & Knowles, 1990).

It has been proposed that the effect of the E165D mutation on the activity of TIM is due to the increased distance from the base to the substrate protons (Straus et al. 1985; Raines et al., 1986; Alagona et al., 1986). The binding constant of the reaction intermediate analog phosphoglycolohydroxamate (PGH) is only slightly reduced by this mutation, implying that substrate is bound in much the same way in both the mutant and wild-type active sites. To determine the effect of the E165D mutation on the structure of the enzyme and on its interaction with substrate and substrate analogs, we have solved and refined the crystal structure of E165D yeast TIM complexed with PGH. We find that the distance from the base to the substrate analog is indeed increased, but that differences in the orientation of catalytic groups in the mutant enzyme may also play a role in the loss of activity.

MATERIALS AND METHODS

Reagents. Glucuronolactone, histidine, streptomycin, ampicillin, reduced nicotinamide adenine dinucleotide, and QAE

† Supported in part by USPHS Grant GM 26788 to G.A.P.

‡ Massachusetts Institute of Technology.
§ Present address: Department of Biological Chemistry and Molecular Pharmacology, Harvard Medical School, Boston, MA 02115.
‖ Department of Biology, Brandeis University.
⊥ Harvard University.
Present address: Department of Chemistry, University of California at San Diego, La Jolla, CA 92093.
△ Departments of Biochemistry and Chemistry, Brandeis University.

• Abstract published in *Advance ACS Abstracts*, February 1, 1994.

0006-2960/94/0433-2824$04.50/0

A

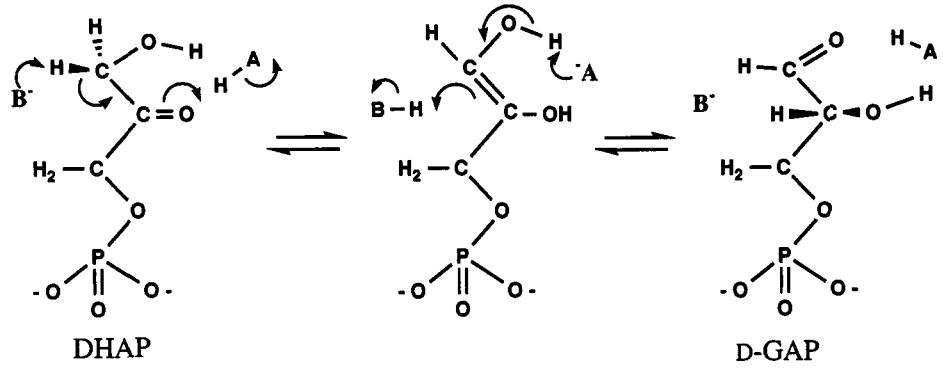

B

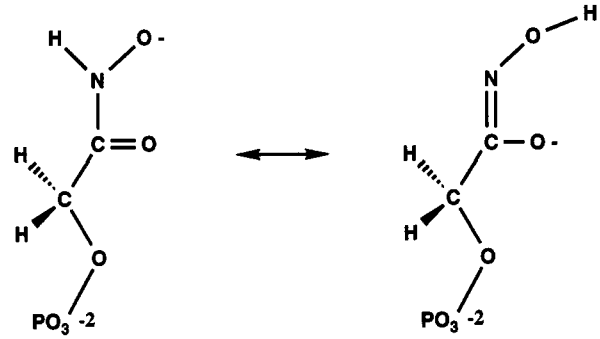

FIGURE 1: (A) Reaction catalyzed by triosephosphate isomerase. It is not certain whether the intermediate is, as indicated, a *cis*-enediol phosphate or instead is actually the two symmetrical *cis*-enediolates. (B) Also shown are the resonance structures of the inhibitor PGH.

Sephadex A-120 were obtained from Sigma Chemical Co. (St. Louis, MO). Poly(ethylene glycol) 4000 was obtained from U.S. Biochemicals (Cleveland, OH). PGH was prepared by J. Belasco. All other reagents were from commercial sources and were used without further purification.

Proteins. The gene for wild-type TIM from yeast was subcloned into a derivative of pBS+/− that has been described (Blacklow & Knowles, 1990). This phagemid vector allowed the efficient production of single-stranded DNA for mutagenesis. The phagemid contains, on an *Eco*RI–*Pst*I fragment, the *trc* promoter upstream from the complete gene for yeast TIM. The mutant in which glutamate 165 was changed to aspartate was constructed by using the oligonucleotide-directed mutagenesis kit available from Amersham (Arlington Hts., IL), which follows the method of Nakamaye and Eckstein (1986). The sequence of the primer used in the mutagenesis reaction was 5′-CCA GAC TGG ATC GTA AGC-3′, which hybridizes to the coding strand of the yeast TIM gene and encodes for the sequence, 5′-GCT TAC GAT CCA GTC TGG-3′, which encodes for the protein sequence, AYDPVW. The sequence of the entire gene was determined to ensure that no other inadvertent mutations were created during mutagenesis. The gene for the mutant protein was subsequently subcloned into the high-expression vector pKK223-3 (Pharmacia LKB, Piscataway, NJ) using the unique *Eco*RI and *Pst*I sites to avoid instability in the phagemid upon large-scale growth. The resulting plasmids contain tandem promoters (*tac* from pKK223-3 and *trc* from the *Eco*RI–*Pst*I phagemid fragment), which allowed the production of 50–80 mg of protein/L of cells. The expression vectors were used to transform *Escherichia coli* strain DF502, which is a *strep*^{R}, *tpi*$^-$ strain that was kindly provided by D. Fraenkel and has been previously described (Straus & Gilbert, 1985).

Large amounts of pure protein were prepared by growing the bacterial transformants in a final volume of 10 L of M63 salts (Miller, 1972) containing casamino acids (0.5%, w/v), glucuronolactone (0.4%, w/v), glycerol (0.1% w/v), $MgSO_4$ (1 mM), thiamine (1 mg/mL), L-histidine (80 mg/L), streptomycin (100 mg/L), and ampicillin (200 mg/L). Cells were harvested after 12–20 h by centrifugation at 3000*g*. The cells were lysed in a continuous flow French pressure cell (Aminco, Urbana, IL), and the lysate was centrifuged at 8500*g* for 1 h to remove cell debris. The ammonium sulfate fraction from 55% to 90% saturation was collected and dialyzed against TE buffer (10 mM Tris-HCl (pH 7.8) and 1 mM EDTA) overnight. The following day, the crude protein was loaded onto a 300-L column of QAE Sephadex A-120 equilibrated with TE buffer and eluted with a linear gradient of 0–300 mM KCl (1 L to 1 L). The proteins were finally purified on a MonoQ 10/10 column using the same gradient. The purity of the proteins was assessed by silver staining overloaded 15% SDS–PAGE gels (Laemmli, 1970). Concentration of the proteins was afforded by Centriprep and Centricon concentration (Amicon, Danvers, MA). The purified E165D mutant TIM protein was dialyzed against 200 mM Tris-HCl (pH 6.8), 1 mM EDTA, and 1 mM β-mercaptoethanol by four changes of buffer in Centricon concentrators.

Crystallization and Initial Characterization. Crystals of the E165D–PGH complex were grown by precipitation from poly(ethylene glycol) 4000 at room temperature in 100-μL portions containing TIM (20 mg/mL, 0.8 mM in active sites)

and PGH (1.5 mM final concentration) in one-half dram vials loosely fitted with cork stoppers. The resulting crystals belonged to the space group $P2_1$, with one dimer in the asymmetric unit and unit cell dimensions of $a = 74.1$ Å, $b = 83.2$ Å, $c = 38.5$ Å, $\beta = 100.0°$. These crystals are isomorphous with those of wild-type yeast TIM crystallized with PGH (Davenport et al., 1991).

X-ray Diffraction Data Collection. All data were collected on a Rigaku AFC-5 rotating anode diffractometer at room temperature. Data were collected in two shells, from infinity to 2.5-Å resolution and from 2.6- to 1.9-Å resolution. A single crystal was used for each data set. Crystal decay was severe in the case of the higher resolution data set, with 35% loss of diffracted intensity by the end of data collection. Because crystals of this mutant proved very difficult to grow, no further data collection was possible. Also, cooling was not a viable option because yeast TIM crystals do not tolerate cooling well. Data were collected by ω scans, and a Lehmann–Larson algorithm was used to compute the background and the background-corrected integrated intensity.

Data Reduction. X-ray radiation damage was estimated by fitting a polynomial equation in time to the loss in intensity of five check reflections. This equation was used to correct all measured intensities. Empirical absorption corrections were applied to the data, as were Lorentz and polarization corrections using standard methods that assume a perfectly mosaic crystal (Stout & Jensen, 1989). Scaling factors between the two data sets were obtained by a comparison of overlapping data, and the merging R factor was 18% for reflections with intensity greater than 2σ.

Structure Determination. An initial electron density map was calculated for the mutant at 2.5-Å resolution using only data from the first crystal. Phases were computed from the refined atomic coordinates of the structure of wild-type yeast TIM with PGH (Davenport et al., 1991), with the atoms of PGH and residue 165 omitted from the calculation. Several rounds of restrained least-squares refinement were carried out first vs the E165D data to remove any "model memory" from the phase angles. To improve the quality of the map, additional refinement was carried out, still with PGH and residue 165 omitted, using the program X-PLOR. Two rounds of X-PLOR refinement with rebuilding in between produced a difference electron density map that gave clear positions for all of the atoms of PGH and Asp-165. This density was too short to accommodate a glutamic acid. PGH and Asp-165 were added to the coordinate set, and a final round of X-PLOR refinement produced an R factor of 24.4% for all data to 2.5-Å resolution.

At this point, the lower and higher resolution data sets were scaled together, resulting in a merged data set that is 56% complete and consists of 19 310 reflections. The 2.03–1.93-Å resolution shell is only 30% complete, while the 2.68–2.46-Å shell is 77% complete. The structure was then refined against all of the data with the program X-PLOR (Brünger et al., 1987), using the lower resolution structure as the initial model. Standard protocols for X-PLOR simulated annealing refinement were used. The model was successively subjected to positional, slow-cooling simulated annealing starting at 3000 K, positional, group B factor, and individual B factor refinement. The WATERHUNTER programs (S. Sugio, R. C. Davenport, and G. A. Petsko, unpublished results) were run using a 2.8-σ difference map cutoff for placing crystallographic waters, and 133 waters were added to the structure. A $3F_o - 2F_c$ electron density map was calculated, and the structure was rebuilt to fit the density. Nine waters were deleted and 14 added. The resulting structure with 138 crystallographic waters was subjected to positional, slow-cooling simulated annealing starting at 2000 K, positional, group B factor, and individual B factor refinement. The R factor dropped from 28.2 to 23.3%.

To eliminate any effect of phase bias from the starting model on the electron density calculated for Asp-165 and PGH, a $2F_o - F_c$ annealed omit map (Hodel et al., 1992) was calculated with Asp-165 and PGH deleted from both subunits. At the 1σ contour level, there was no density for part of the main chain of Asp-165 in subunit one and the side chain in subunit two or for part of the PGH in subunit one. Also, there appeared to be an additional water in the subunit one active site; in the subunit two active site, it was unclear whether another water could be added, and as a result the side chain of Ser-96 moved. To improve the map, extensive positional refinement was carried out on this model structure with Ser-96, Asp-165, and PGH deleted from both subunits. A $3F_o - 2F_c$ map, extending over a box around the dimer and calculated using the omit refined model, showed density for Asp-165 and PGH in both subunits. Ser-95, Asp-165, and PGH were built in, and then the structure was subjected to positional, group B factor, and individual B factor refinement, causing the R factor to drop from 27.3% to 23.8%. A $2F_o - F_c$ map was calculated, and a water hydrogen bonding to the Asp-165 in subunit one was added. This structure was subjected to further positional, slow-cooling simulated annealing starting at 2000 K, positional, group B factor, and individual B factor refinement to a final R factor of 22.5% vs all data. The accumulated R factor varies smoothly with resolution and is 20.8% when only the data to 2.25-Å resolution are included, 19.2% to 2.67-Å resolution, and 18.0% to 3.04-Å resolution. When weak reflections with $I/\sigma(I) \leq 1.0$ are excluded, the overall R factor to 2 Å is 19.4%. Although the structure is nominally at 2-Å resolution, the quality of the data beyond 2.3 Å is not high. Therefore, even though the starting model has been refined at high resolution and all data have been included, this is not a high-resolution structure.

RESULTS AND DISCUSSION

Although the limited number of crystals available and the use of a diffractometer to collect data limited the quantity and quality of the data that could be collected, the electron density maps calculated for the mutant structure were clear and easy to interpret (Figure 2). There are probably two reasons for this. First, the phases were calculated from a well-refined protein structure, that of the wild-type enzyme complexed with PGH. Second, the change in the structure due to the mutation is small.

The geometry of the structure is reasonable. The root-mean-square (rms) deviation from ideality is 0.02 Å for bonds, 4.39° for bond angles, 26.21° for dihedral angles, and 2.00° for improper dihedral angles. There are 83 bond deviations greater than 0.06 Å (the largest is 0.12 Å), 171 angle deviations greater than 10° (the largest is 21.96°), no dihedral deviations greater than 90°, and no improper deviations greater than 20°. None of the large deviations involves active-site residues. There is only one nonbonded distance of less than 3 Å that is not a hydrogen bond, and this is far from the active site (the Pro-33 γ-carbon to Ala-136 carbonyl oxygen distance is 2.9 Å). In general, the geometric parameters for subunit two are slightly worse than those for subunit one; this is always observed for yeast TIM structures and probably reflects looser intermolecular packing around the second subunit.

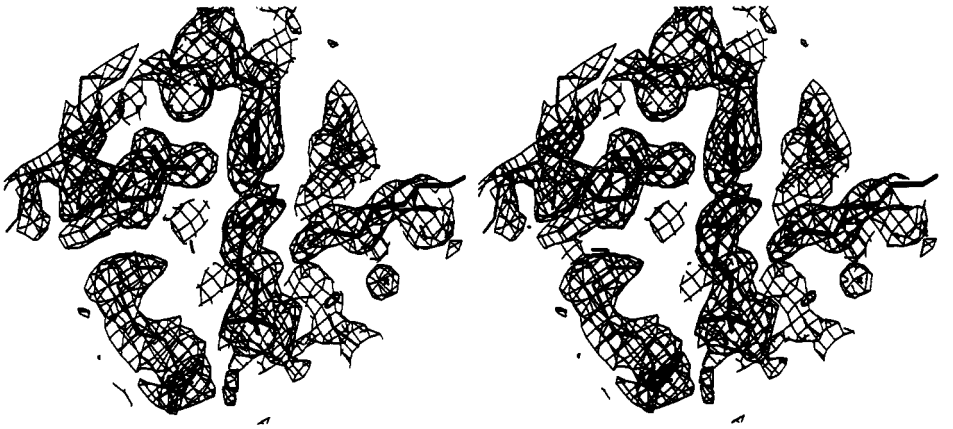

FIGURE 2: Electron density for the E165D TIM–PGH complex subunit one active site. Residues Lys-12, His-95, Asp-165, and PGH are shown in thick black lines in a $2F_o - F_c$ map, contoured at 1σ.

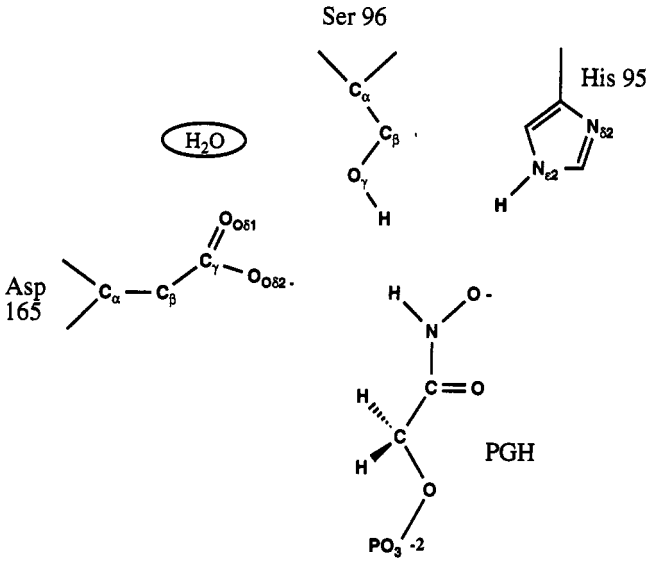

FIGURE 3: Schematic representation of the E165D TIM–PGH complex active site. The protonation state of the PGH is uncertain.

We see differences between subunits one and two of the E165D structure, but cannot be sure whether these are simply due to the relatively poorer quality of the density in subunit two. Since the dimer is the asymmetric unit and the environments of the two monomers are different, the effect that conformational heterogeneity of active-site residues might have on the catalytic activity of the mutant is difficult to estimate. However, since proton transfer is rate-limiting for this mutant, and since Asp-165 is the residue that carries out this transfer (Raines & Knowles, 1986), conformational disorder in Asp-165 may play a role.

In both subunits, the carboxylate of Asp-165 is positioned such that the *anti* orbital would be utilized for proton abstraction from the substrate, in contrast to the wild-type enzyme in which the *syn* orbital of the carboxylate of Glu-165 is used (see Figure 3). Furthermore, although the carboxylate oxygens of Asp-165 are in somewhat similar positions in both subunits, the paths by which they arrive there are different. In subunit one, $\phi = -124.0°$, $\psi = 100.2°$, $\chi_1 = 55.6°$, and $\chi_2 = -56.4°$, while in subunit two, $\phi = -128.1°$, $\psi = 72.5°$, $\chi_1 = 178.3°$, and $\chi_2 = 53.9°$. Neither of these Asp conformations is close to the most common conformer for Asp that has been determined by Ponder and Richards (1987). When subunits one and two are superposed (Figure 4), the overall main-chain rms difference is 1.1 Å, and the distance between Asp-165 Oδ2 atoms is 0.9 Å and Oδ1 atoms is 2.8 Å. In subunit one, there is a water molecule (Wat-688 in Figure 4) that is hydrogen bonded to Asp-165 Oδ1 (3.9 Å), the carbonyl oxygen (3.5 Å), and the main-chain nitrogens of Ile-127 (3.3 Å) and Gly-128 (3.2 Å). This water is either missing or has a lower occupancy in subunit two. (There is some density at 0.5σ in the $3F_o - 2F_c$ omit map at this location in subunit two.) Perhaps as a consequence of this "missing" water, Ser-96 in subunit two is shifted away from the PGH and toward the location of the water in subunit one. In subunit two, Ser-96 Oγ is hydrogen-bonded to Asp-165 O, and Ser-96 N is hydrogen-bonded to Asp-165 Oδ2, while in subunit one, Ser-96 Oγ makes a bifurcated hydrogen bond to Glu-97 N and His-95 Nδ1, and Asp-165 N is hydrogen-bonded to Asp-165 Oδ1. The disorder in Asp-165 is apparent from the weaker electron density in subunit two for the side chain and the conformational difference with subunit one. This disorder may play a role in the low activity of the mutant. The ensuing discussion of the structure–activity relation for this mutant will be based primarily on the picture of the active site in subunit one, as this is the clearer of the two images.

Overall, the structure of the mutant protein is unchanged from that of the wild-type, and the detailed structure of the active site is largely preserved. When the E165D mutant structure is superimposed on the wild-type yeast TIM–PGH complex structure (Davenport et al., 1991), the subunit one main-chain rms difference is only 0.6 Å. The positions of the inhibitor PGH and the active-site residues His-95, Lys-12, and Glu-97 are the same in both structures. The position of Ser-96, however, is somewhat different in the two structures. In the mutant structure, the Ser-96 side chain points down toward Asp-165, while in the wild-type PGH complex structure it points up and away from the active site. This difference is not entirely surprising, considering that Ser-96 is in a different conformation in the wild-type liganded and wild-type unliganded structures (Davenport et al., 1991; Lolis et al., 1990). It is more surprising that the position of Ser-96 in this mutant liganded structure is closer to its position in the wild-type *un*liganded structure than in the wild-type liganded structure. In fact, the average of the Ser-96 position in subunits one and two of the mutant is approximately the same as that of Ser-96 in the wild-type unliganded structure. As a possible consequence of this movement, Asp-165 takes up a position in the mutant structure that is different from that of Glu-165; its position is intermediate between the Glu-165 positions in the wild-type liganded and unliganded structures (see Figure 5). Furthermore, in the wild-type PGH complex structure, there are two water molecules in between Ser-96 and Glu-165 that are replaced by one water molecule in subunit one of the mutant complex structure (Figure 5) (Davenport et al., 1991).

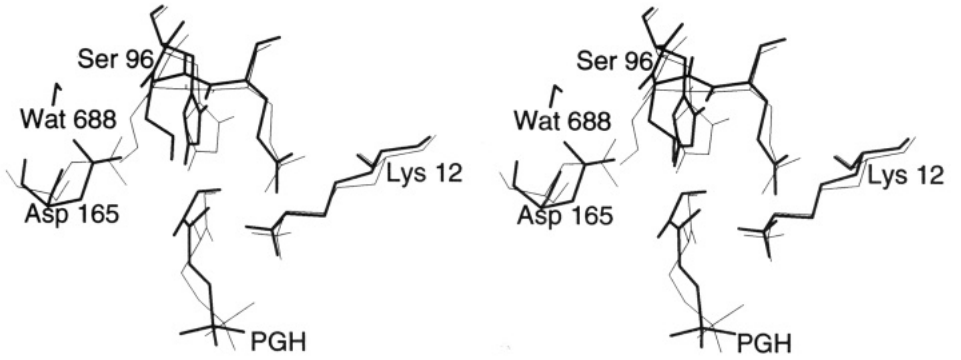

FIGURE 4: Least-squares superposition of subunits one and two main-chain atoms of the E165D mutant–PGH complex structure. Subunit one active-site residues are shown in thick black lines and subunit two's are in thin black lines.

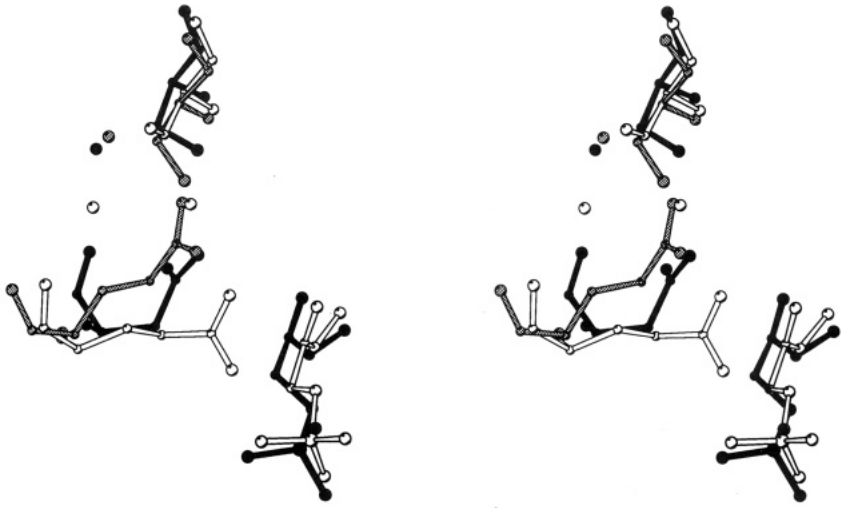

FIGURE 5: Superposition of subunit one main-chain atoms of the mutant liganded structure and the wild-type liganded and unliganded structures. Shown are residues Ser-96 and Asp/Glu-165 and the inhibitor PGH, drawn using the program MOLSCRIPT (Kraulis, 1991). The mutant structure is colored in black, the liganded wild-type structure is white, and the unliganded wild-type structure is shaded gray.

In the wild-type unliganded structure there is also only one water at this location, and the Glu-165 carboxylate exactly overlaps with one of the two waters in the wild-type liganded structure (Lolis et al., 1990).

It is also evident from Figure 5 that the distance from the carboxylate of the catalytic base to the inhibitor is significantly increased in the mutant. The distances from the carboxylate oxygens of the catalytic base to the PGH nitrogen and carbonyl carbon are given in Table 1. In the wild-type structure, both carboxylate oxygens interact strongly with substrate, whereas in the mutant only one oxygen interacts, and this only weakly. In spite of the difference in the conformation of Asp-165 in the two subunits of the mutant structure, the relevant carboxylate–inhibitor distances are essentially identical in each subunit. In subunit one of the mutant the Oδ2 Asp-165 carboxylate oxygen interacts with substrate, while in subunit two the Oδ1 oxygen is involved; this result suggests that either of these oxygens may be used to abstract a proton from the substrate. (The chemically equivalent carboxylate oxygens are labeled such that the Oδ2 atoms are closest together when the two subunits are superimposed.) The wild-type structure suggests that a bidentate proton-transfer mechanism may occur, whereby a bidentate base (both oxygens of the carboxylate of Glu-165) attacks the bidonor substrate (shuttling the proton from C1 to C2 of the substrate). If the structure of the E165D TIM–PGH complex presents an accurate view of the interactions of Asp-165 and the substrate, then proton transfer in the mutant must proceed by a different path that involves only one of the carboxylate oxygens. Alternatively, in the wild-type enzyme the catalytic base Glu-165 is positioned so that the reaction can proceed easily in either direction (transferring the proton from C1 to C2 or from C2 to C1), depending on which substrate is present in the active site. In the mutant enzyme, movement of the carboxylate of Asp-165 would be required at some point during the reaction.

Table 1: Distances of the Carboxylate Oxygens of Catalytic Base to Substrate

oxygen	distance to PGH nitrogen (Å)	distance to PGH carbonyl carbon (Å)
E165D, subunit one		
Oδ1	5.7	5.8
Oδ2	4.4	4.1
E165D, subunit two		
Oδ1	4.4	3.9
Oδ2	6.0	5.6
wild-type, subunit one		
Oε1	2.8	3.4
Oε2	3.1	3.6

Certainly, the increase in the distance between the Asp-165 carboxylate and the PGH of about 1 Å compared to the wild-type enzyme must be an important factor affecting the catalytic activity of the mutant. The change in the orientation of the carboxylate relative to the substrate is probably also significant. The existence of alternative conformations for Asp-165 and the position of bound water molecules in the active site may also have an effect, but these factors are harder to evaluate. The structure reported here represents a picture of the "parent" mutant for a series of genetically selected pseudorevertants of high catalytic potency, in which second site suppressor changes can partially compensate for the E165D

lesion (Blacklow & Knowles, 1990). It will be important to compare this structure to those of various pseudorevertant enzymes to obtain a more complete understanding of the various factors that make Glu-165 an effective proton-transfer catalyst in wild-type triosephosphate isomerase.

ACKNOWLEDGMENT

We thank Jeremy Knowles for advice and careful reading of the manuscript, Karen Allen for helpful discussions, Ilme Schlichting for help with the initial refinement, and Xidong Xhang, Shigetoshi Sugio, and Dagmar Ringe for communicating results prior to publication.

REFERENCES

Alagona, G., Ghio, C., & Kollman, P. A. (1986) Simple model for the effect of glu 165 to asp 165 mutation on the rate of catalysis in triose phosphate isomerase. *J. Mol. Biol. 191*, 23–27.

Alber, T., Banner, D. W., Bloomer, A. C., Petsko, G. A., Phillips, D. C., Rivers, P. S., & Wilson, I. A. (1981) On the three-dimensional structure and catalytic mechanism of triosephosphate isomerase. *Philos. Trans. R. Soc. London B 293*, 159–171.

Alber, T., Davenport, R. C., Jr., Giammona, D. A., Lolis, E., Petsko, G. A., & Ringe, D. (1987) Crystallography and site-directed mutagenesis of yeast triosephosphate isomerase: What can we learn about catalysis from a "simple" enzyme? *Cold Spring Harbor Symp. Quant. Biol. LII*, 603–613.

Albery, W. J., & Knowles, J. R. (1976a) Free-energy profile for the reaction catalyzed by triosephosphate isomerase. *Biochemistry 15*, 5627–5631.

Albery, W. J., & Knowles, J. R. (1976b) Evolution of enzyme function and the development of catalytic efficiency. *Biochemistry 15*, 5631–5640.

Belasco, J. G., & Knowles, J. R. (1980) Direct observation of substrate distortion by triosephosphate isomerase using transform infrared spectroscopy. *Biochemistry 19*, 472–477.

Blacklow, S. C., & Knowles, J. R. (1990) How can a catalytic lesion be offset? The energetics of two pseudorevertant triosephosphate isomerases. *Biochemistry 29*, 4099–4108.

Blacklow, S. C., Raines, R. T., Lim, W. A., Zamore, P. D., & Knowles, J. R. (1988) Triosephosphate isomerase catalysis is diffusion controlled. *Biochemistry 27*, 1158–1167.

Brünger, A. T., Kuriyan, J., & Karplus, M. (1987) Crystallographic R-factor refinement by molecular dynamics. *Science 235*, 458–460.

Davenport, R. C., Bash, P. A., Seaton, B. A., Karplus, M., Petsko, G. A., & Ringe, D. (1991) Structure of the triosephosphate isomerase–phosphoglycolohydroxamate complex: An analogue of the intermediate on the reaction pathway. *Biochemistry 30*, 5821–5826.

Hartman, F. C. (1968) Irreversible inactivation of triose phosphate isomerase by 1-hydroxy-3-iodo-2-propanone phosphate. *Biochem. Biophys. Res. Commun. 33*, 888–894.

Hermes, J. D., Blacklow, S. C., & Knowles, J. R. (1987) The development of enzyme catalytic efficiency: An experimental approach. *Cold Spring Harbor Symp. Quant. Biol. LII*, 597–602.

Hodel, A., Kim, S.-H., & Brünger, A. T. (1992) Model bias in macromolecular crystal structures. *Acta Crystallogr. A 48*, 851–858.

Joseph-McCarthy, D., Lolis, E., Komives, E. A., & Petsko, G. A. (1994) Crystal structure of the K12M/G15A triosephosphate isomerase double mutant and electrostatic analysis of the active site. *Biochemistry* (preceding article in this issue).

Knowles, J. R. (1991) Enzyme catalysis: Not different, just better. *Nature 350*, 121–124.

Knowles, J. R., & Albery, W. J. (1977) Perfection in enzyme catalysis: The energetics of triosephosphate isomerase. *Acc. Chem. Res. 10*, 105–111.

Komives, E. A., Chang, L. C., Lolis, E., Tilton, R. F., Petsko, G. A., & Knowles, J. R. (1991) Electrophilic catalysis in triosephosphate isomerase: the role of histidine 95. *Biochemistry 30*, 3011–3019.

Kraulis, P. J. (1991) MOLSCRIPT: A program to produce both detailed and schematic plots of protein structures. *J. Appl. Crystallogr. 24*, 946–950.

Laemmli, U. K. (1970) Cleavage of structural proteins during the assembly of the head bacteriophage T4. *Nature 227*, 680–685.

Lodi, P. J., & Knowles, J. R. (1993) Direct evidence for the exploitation of an α-helix in the catalytic mechanism of triosephosphate isomerase. *Biochemistry 32*, 4338–4343.

Lolis, E., Alber, T., Davenport, R. C., Rose, D., Hartman, F. C., & Petsko, G. A. (1990) Structure of yeast triosephosphate isomerase at 1.9 Å resolution. *Biochemistry 29*, 6609–6618.

Miller, J. H. (1972) *Experiments in Molecular Genetics*, Cold Spring Harbor Laboratory Press, Cold Spring Harbor, NY.

Nakamaye, K. L., & Eckstein, F. (1986) Inhibition of restriction endonuclease Nci I cleavage by phosphothioate groups and its application to oligonucleotide-directed mutagenesis. *Nucleic Acids Res. 14*, 9679–9698.

Phillips, D. C., Sternberg, M. J. E., Thornton, J. M., & Wilson, I. A. (1977) An analysis of the three-dimensional structure of chicken triosephosphate isomerase. *Biochem. Soc. Trans. 5*, 642–647.

Ponder, J. W., & Richards, F. M. (1987) Tertiary templates for proteins: Use of packing criteria in the enumeration of allowed sequences for different structural classes. *J. Mol. Biol. 193*, 775–791.

Raines, R. T., & Knowles, J. R. (1986) The mechanistic pathway of a mutant triosephosphate isomerase. *Ann. N.Y. Acad. Sci. 471*, 266–271.

Raines, R. T., Straus, D. R., Gilbert, W., & Knowles, J. R. (1986) The kinetic consequences of altering the catalytic residues of triosephosphate isomerase. *Philos. Trans. R. Soc. London A 317*, 371–380.

Stout, G. H., & Jensen, L. H. (1989) *X-ray structure determination: A practical guide*, John Wiley & Sons, New York.

Straus, D., & Gilbert, W. (1985) Chicken triosephosphate isomerase complements an *Escherichia coli* deficiency. *Proc. Natl. Acad. Sci. U.S.A. 82*, 2014–2018.

Straus, D., Raines, R. T., Kawashima, E., Knowles, J. R., & Gilbert, W. (1985) Active site of triosephosphate isomerase: In vitro mutagenesis and characterization of an altered enzyme. *Proc. Natl. Acad. Sci. U.S.A. 82*, 2272–2276.

Webb, M. R., & Knowles, J. R. (1974) The existence of an electrophilic component in the reaction catalyzed by triosephosphate isomerase. *Biochem. J. 141*, 589–592.